Supplementary Information

MPI Performance of Magnetic Nanoparticles Depends on Matrix Composition and Temperature: Implications for in Vivo MPI Signal Amplitude and Spatial Resolution

Marzieh Salimi [a,b], Wenshen Wang[a,c], Stéphane Roux[d], Gautier Laurent[d], Rana Bazzi[d], Patrick Goodwill[e], Guanshu Liu[a,c], Jeff WM Bulte[a-c,f,h]*

Transmission electron microscopy of MNPs

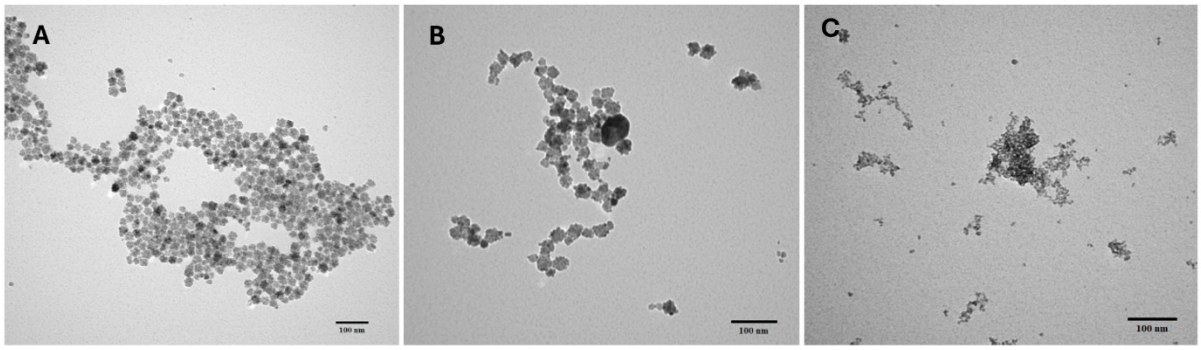

Supplementary Figure 1. Transmission Electron Microscopy (TEM) images of (**A**) NF, (**B**) GIONF, and (**C**) ferucarbotran MNP formulations used in this study. Scale bars represent 100 nm.

Physicomagnetic properties of MNPs

Supplementary Table 1. Physicomagnetic characterization of NF, GIONF, and ferucarbotran.

MNP	Core size (nm) from TEM	Hydrodynamic size (nm) from DLS	Saturation magnetization M_s (emu.g^{-1}) *	Susceptibility χ *
NF	43.9	177±64	69	128
GIONF	50	160±76	69	128
Ferucarbotran	14.2	69±29	96	0.135

*Extracted from references [1-3].

[a.] *Russell H. Morgan Department of Radiology and Radiological Science, Division of MR Research, the Johns Hopkins University, Baltimore, Maryland, USA.*
[b.] *Cellular Imaging Section and Vascular Biology Program, the Johns Hopkins University School of Medicine, Baltimore, Maryland, USA.*
[c.] *F.M. Kirby Research Center for Functional Brain Imaging, Kennedy Krieger Inc., Baltimore, MD, USA.*
[d.] *Université de Franche-Comté, CNRS, Chrono-environnement, F-25000, Besançon, France.*
[e.] *Magnetic Insight Inc. Alameda, CA, USA*
[f.] *Department of Biomedical Engineering, the Johns Hopkins University School of Medicine, Baltimore, Maryland, USA.*
[g.] *Department of Oncology, the Johns Hopkins University School of Medicine, Baltimore, Maryland, USA.*
[h.] *Department of Chemical & Biomolecular Engineering, Johns Hopkins University Whiting School of Engineering.*
* *Corresponding author email: jwmbulte@mri.jhu.edu.*

MNP signal amplitude and FWMH values of MNPs

Supplementary Table 2. Signal amplitude and FWHM values for different MNPs in water (0% gelatin or 0% BSA).

MNP	Concentration (µg/mL)	Quantity (µg)	Signal amplitude (a.u.)	SD	FWHM (mT)	SD
NF	25	12.5	1.28	0.29	12	0.1
	50	25	2.8	0.27	11	0.3
	100	50	4.33	0.59	12	1.5
GIONF	25	12.5	1.42	0.01	12	0.04
	50	25	2.74	0.01	12	0.1
	100	50	4.4	0.02	14	0.1
Ferucarbotran	25	12.5	0.68	0.01	11	0.1
	50	25	1.26	0.04	11	1.3
	100	50	2.74	0.03	12	0.03
GIONF*	50	5	0.51	0.02	10	0.2
Ferucarbotran*	100	10	0.62	0.02	13	0.4

*Baseline measurements in water (0% BSA content).

Compressibility error calculations

When a "quantity" depends on measured variables, the uncertainty (standard deviation) in the quantity can be estimated by considering how sensitive the quantity is to changes in those variables, and then combining the uncertainties in the variables [4, 5].

Compressibility formula

The compressibility β_s is given by:

$$\beta_s = \frac{1}{C^2 \times \rho} \quad (1)$$

Where C is the velocity and ρ is the density.

Error propagation

For a function $\beta_s(C, \rho)$, the uncertainty in β_s due to uncertainties in C and ρ can be estimated using the partial derivatives with respect to each variable:

$$\sigma_{\beta_s}^2 = (\frac{\partial \beta_s}{\partial C})^2 \sigma_C^2 + (\frac{\partial \beta_s}{\partial \rho})^2 \sigma_\rho^2 \quad (2)$$

where σ_C is the standard deviation in velocity and σ_ρ is the standard deviation in density.

Partial derivatives

1. The partial derivative with respect to C is:

$$\frac{\partial \beta_s}{\partial C} = \frac{\partial}{\partial C}\left(\frac{1}{C^2 \times \rho}\right) = -\frac{2}{C^3 \times \rho} \quad (3)$$

2. The partial derivative with respect to ρ is:

$$\frac{\partial \beta_s}{\partial \rho} = \frac{\partial}{\partial \rho}\left(\frac{1}{C^2 \times \rho}\right) = -\frac{2}{C^2 \times \rho^2} \quad , \quad \frac{\partial \beta_s}{\partial \rho} = \frac{\partial}{\partial \rho}\left(\frac{1}{C^2 \times \rho}\right) = -\frac{1}{C^2 \times \rho^2} \quad (4)$$

Simplifying for dominant contribution:

Given the typical situation where the uncertainty in velocity σ_C is much more significant than the uncertainty in density σ_ρ, the term involving σ_ρ is often negligible. Hence, the primary contribution to $\sigma_{\beta s}$ comes from the uncertainty in C.

Thus, we approximate:

$$\sigma_{\beta_s} \approx \left|\frac{\partial \beta_s}{\partial C}\right| \sigma_c = \left|\frac{-2}{C^3 \times \rho}\right| \sigma_c = \frac{2 \times \sigma_c}{C^3 \times \rho} \quad (5)$$

Final formula

The formula used for the standard deviation of compressibility is:

$$\sigma_{\beta_s} = \frac{2 \times \sigma_c}{C^3 \times \rho} \quad (6)$$

This formula allows an estimation of how the uncertainty in the velocity σ_C propagates into uncertainty in the calculated compressibility β_s. In here, C is the average measured velocity and σ_C is the standard deviation of these velocity measurements, reflecting the variability or uncertainty in the velocity data.

When measuring the velocity multiple times, the average velocity C and the spread of those measurements around the average can be calculated, yielding the standard deviation σ_C . This standard deviation quantifies how much the individual velocity measurements differ from the average value. In the error propagation formula for compressibility β_s, σ_C was used to estimate how the uncertainty in the velocity measurements affects the uncertainty in the calculated compressibility.

Viscosity mesurements of gelatin and BSA

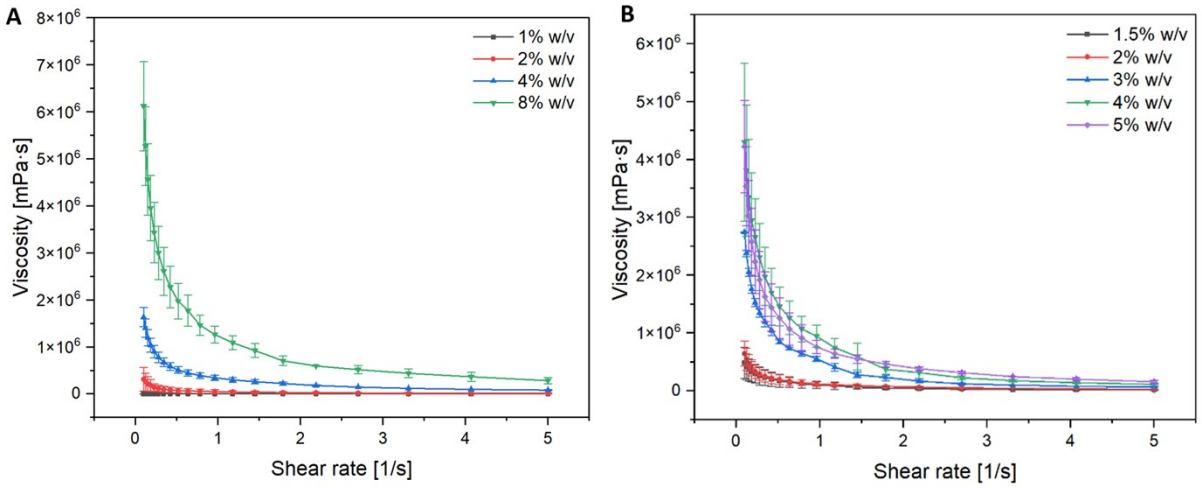

Supplementary Figure 2. Viscosity measurements of (**A**) gelatin and (**B**) BSA hydrogel samples at various concentrations. Both sets of hydrogel samples exhibit shear-thinning behavior, where viscosity decreases as the shear rate increases. Error bars represent standard deviations across triplicate measurements.

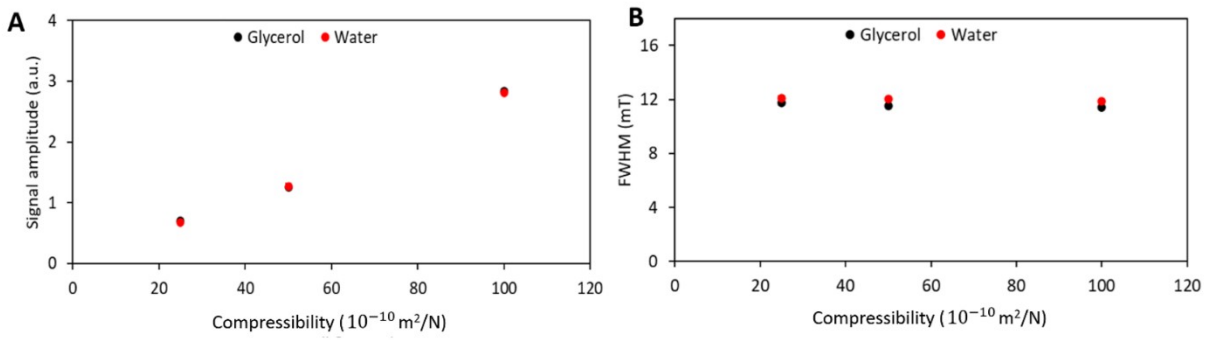

Supplementary Figure 3. (A) MPI signal amplitude and **(B)** FWHM values for ferucarbotran at different concentrations (25, 50, and 100 µg/mL) in glycerol and water. Data were obtained at room temperature and are shown as mean±SD for three independent experiments.

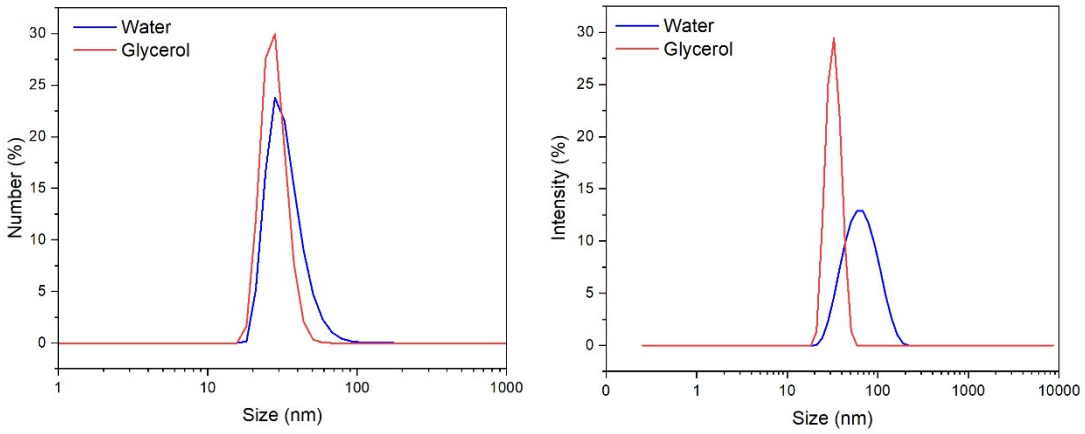

Hydrodynamic size of ferucarbotran in glycerol and water

A **B**

Supplementary Figure 4. Number-based (**A**) and intensity-based (**B**) hydrodynamic size distribution of ferucarbotran in glycerol and water.

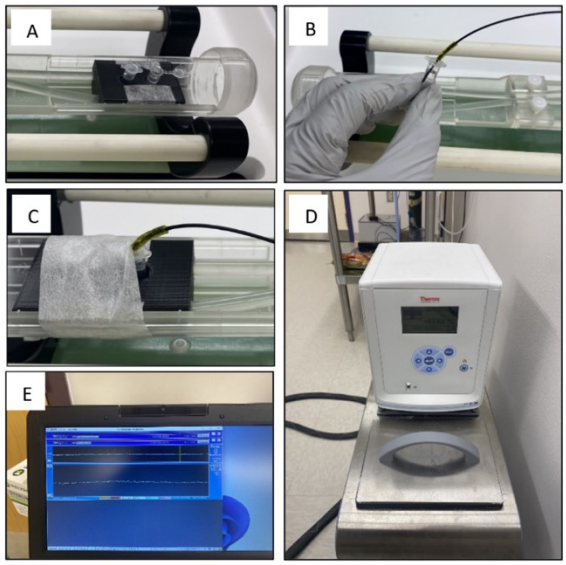

Supplementary Figure 5. Experimental setup for measurement of the MPI signal amplitudes of ferucarbotran (100 µg Fe/mL) at different temperatures (10-55 ℃). **(A)** Holder containing ferucarbotran and water vials, allowing water to flow in and out to regulate temperature. **(B)** A thermocouple thermometer inserted into the water vial to monitor the temperature of ferucarbotran indirectly. **(C)** Vials are secured in the holder for stable temperature control. **(D)** Water pump used to circulate water at different temperatures for precise regulation of the experimental conditions. **(E)** Real-time temperature monitoring display provides continuous tracking of temperature changes over time.

References

1. Hugounenq, P., et al., *Iron oxide monocrystalline nanoflowers for highly efficient magnetic hyperthermia.* The Journal of Physical Chemistry C, 2012. **116**(29): p. 15702-15712.
2. Nicolás-Boluda, A., et al., *Photothermal depletion of cancer-associated fibroblasts normalizes tumor stiffness in desmoplastic cholangiocarcinoma.* ACS nano, 2020. **14**(5): p. 5738-5753.
3. Ota, S., et al., *Effect of particle size and structure on harmonic intensity of blood-pooling multi-core magnetic nanoparticles for magnetic particle imaging.* Int. J. Magn. Part. Imaging, 2017. **3**(1): p. 1703003.
4. Skoog, D.A., F.J. Holler, and S. Crouch, *Principles of instrumental analysis. Thomson Brooks.* Cole, Canada, 2007.
5. Neuhauser, C. and M.L. Roper, *Calculus for biology and medicine*. 2004: Pearson/Prentice Hall Upper Saddle River, NJ.